Controlling Fe nanocrystallization in amorphous Fe 86 Zr 7 Cu 1 B 6 by linear varying current Joule heating

F. C. S. da Silva, E. F. Ferrari, M. Knobel, I. L. Torriani, and D. R. dos Santos

Citation: Applied Physics Letters **77**, 1375 (2000); doi: 10.1063/1.1290049

View online: http://dx.doi.org/10.1063/1.1290049

View Table of Contents: http://scitation.aip.org/content/aip/journal/apl/77/9?ver=pdfcov

Published by the AIP Publishing

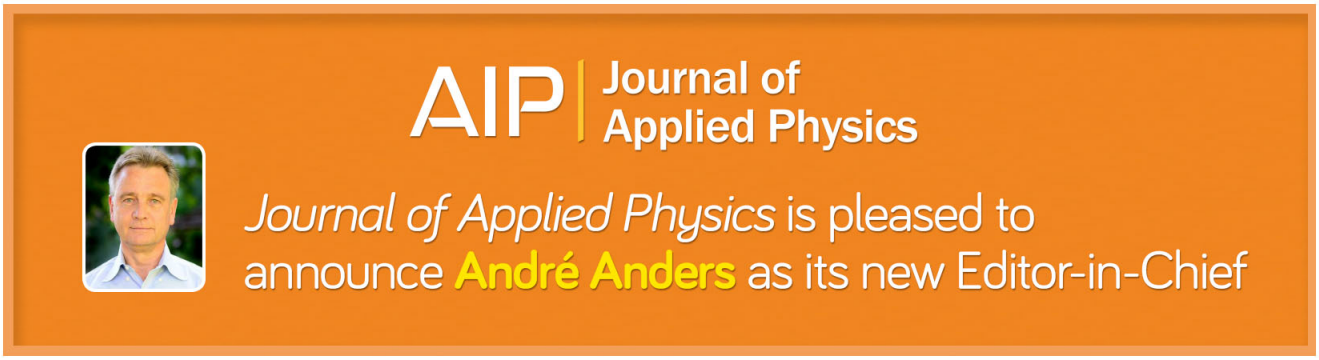

Controlling Fe nanocrystallization in amorphous $Fe_{86}Zr_7Cu_1B_6$ by linear varying current Joule heating

F. C. S. da Silva,[a] E. F. Ferrari, M. Knobel, I. L. Torriani, and D. R. dos Santos[b]
Instituto de Física ''Gleb Wataghin,'' Universidade Estadual de Campinas (UNICAMP), CP 6165, 13083-970, Campinas, São Paulo, Brazil

(Received 4 May 2000; accepted for publication 5 July 2000)

Amorphous melt-spun $Fe_{86}Zr_7Cu_1B_6$ ribbons were annealed using the linear varying current Joule heating method. Experimental curves of resistance (R) and temperature (T) versus applied current (I) allow one to follow precisely the crystallization of $\alpha-$Fe nanoparticles during annealing. This result proves that the applied current can be considered a reliable parameter to control the crystalline fraction in this alloy. A comparison between structural and magnetic measurements shows that the $R(I)$ curve can be used as a guide to identify a condition for optimum soft magnetic properties of this alloy. © *2000 American Institute of Physics.* [S0003-6951(00)02035-0]

Linear varying current Joule heating (LVC–JH) is a variation of the so called dc Joule heating method[1] commonly used to anneal metallic samples. Typically, the applied electrical current I varies linearly up to a final value I_{final} instead of being abruptly raised from zero to I_{final}. The main advantage of the LVC–JH is that the sample's structural transformations can be easily followed through the resistance versus current $R(I)$ curve. Recently, it was experimentaly demonstrated that the $R(I)$ curve can be used to control the fraction of precipitated Co in binary Cu–Co alloys.[2,3] In this work we assert that the $R(I)$ curve can be used to precisely control the crystalline fraction of Fe in amorphous $Fe_{86}Zr_7Cu_1B_6$ alloy. As an example, we used this method to find an optimum annealing condition for the soft magnetic properties of this system.

Ribbon strips of $Fe_{86}Zr_7Cu_1B_6$ were produced by melt spinning. The dimensions of all samples were 2.73 mm width, $\approx 25\,\mu$m thick, and 10.0 cm long. All samples were annealed using the LVC–JH in a 10^{-4} mbar vacuum. The four-probe setup consisted of two pairs of U-shaped electrical contacts also used to clamp the sample within a small region in order to minimize conductive thermal losses. Online annealing temperature was measured using a chromel–alumel thermocouple with small contact area ($\approx 0.01\,\text{mm}^2$) attached on the sample's surface. The applied current I was varied step-by-step with an increment $\delta I = 0.03$ A, and waiting time $\delta t = 10$ s between steps. After reaching the final annealing value, the applied current was always decreased down to zero by abrupt interruption (quenching). X-ray diffraction (XRD) measurements made on the annealed samples were performed by a Philips PW 1840 diffractometer in the $\Theta-2\Theta$ configuration (Cu $K\alpha$ radiation). Hysteresis curves were obtained using a homemade hysteresis loop tracer.

Figure 1(a) shows typical $R(I)$, and $T(I)$ curves measured during annealing of an as-cast $Fe_{86}Zr_7Cu_1B_6$ sample with the LVC–JH. The $R(I)$ curve displays a first minimum at about $I = I_{1\text{st min}} = 0.25$ A, after which a slow increase in R is observed. After a maximum at $I = I_{\max} = 1.2$ A, the resistance drops down to a second minimum at $I_{2\text{nd min}} \approx 2.0$ A where it turns to increase again up to the sample's melting point at $I > 3.0$ A. This behavior was observed in more than 100 annealed samples in the same conditions. The only observed fluctuations in the current and resistance values appeared at the critical points. These fluctuations are mainly related to geometrical factors such as sample's average thickness and width. Figure 1(a) shows that temperature always

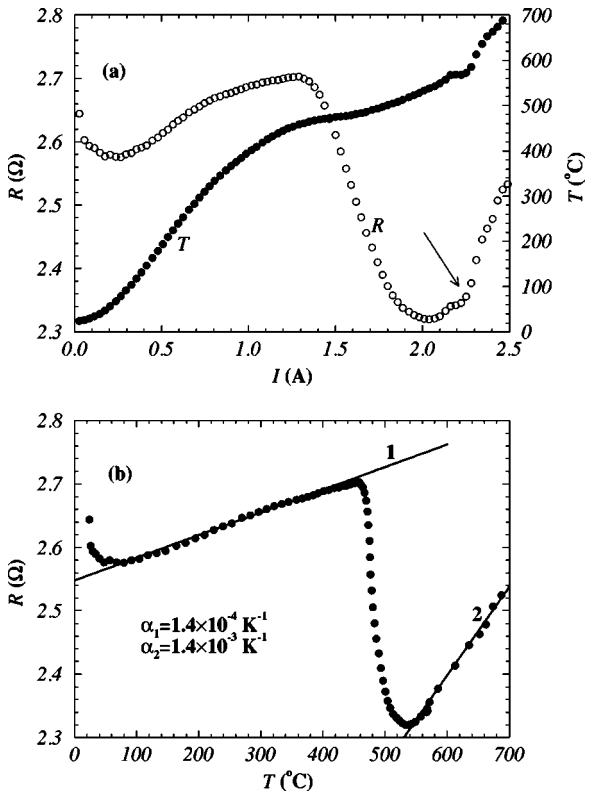

FIG. 1. (a) Resistance and temperature vs annealing current using the linear varying current Joule heating method for an as cast $Fe_{86}Zr_7Cu_1B_6$ sample. Curve (b) is obtained by crossing the y axes in (a). The arrow indicates the point of best soft magnetic properties.

[a]Electronic mail: fcss@ifi.unicamp.br
[b]Present address: Universidade Estadual do Norte Fluminense Rio de Janeiro, Brazil.

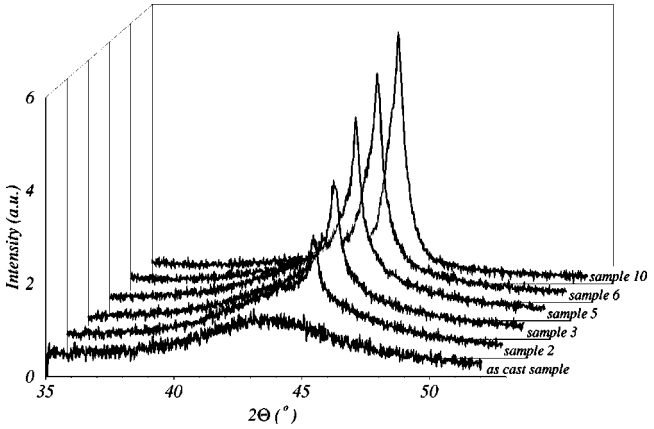

FIG. 2. XRD measurements $Fe_{86}Zr_7Cu_1B_6$ samples annealed by the linear varying current Joule heating method at different values of I_{final}.

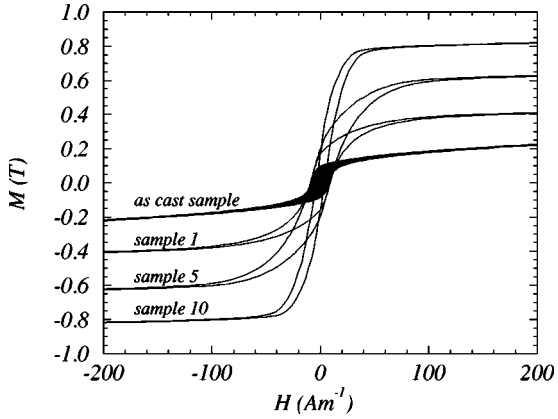

FIG. 3. Room temperature hysteresis loops of $Fe_{86}Zr_7Cu_1B_6$ samples with different crystalline fractions (see Table I).

increases with the annealing current even during the resistance drop. In fact this is a consequence of a positive heating balance between the Joule power (I^2R) and the radiative loss.

Crossing both $R(I)$ and $T(I)$ curves, one obtains Fig. 1(b) which is similar to the $R(T)$ curve obtained using conventional furnace annealing.[4] The first minimum at $T \approx 60\,^{\circ}\text{C}$ (close to the ferromagnetic–paramagnetic transition of the amorphous phase) is possibly related to the scattering produced by the existence of low density spin clusters in a higher density ferromagnetic matrix.[5] After the first minimum, a typical metallic behavior, well described by the equation $R = R_o[1 + \alpha(T - T_o)]$, is observed. Here, $\alpha_1 = 1.4 \times 10^{-4}\,\text{K}^{-1}$, T_o, and R_o are the thermal coeficient of resistance (TCR), the initial annealing temperature, and its corresponding resistance value, respectively. A maximum in R occurs at $T = T_{\max} = 450\,^{\circ}\text{C}$. $T_{\max}$ matches the value at which primary crystallization of $\alpha - \text{Fe}$ particles starts.[4] Fe crystallization reduces the resistance down to a second minimum at $530\,^{\circ}\text{C}$ where the effect is overcome by a new metallic behavior ($\alpha_2 = 1.4 \times 10^{-3}\,\text{K}^{-1}$) approaching that of pure crystalline Fe ($\alpha_{\text{Fe}} = 5 \times 10^{-3}\,\text{K}^{-1}$).

Taking the $R(I)$ curve as a guide, we prepared 12 samples using the LVC–JH. They were annealed up to a final current ($I_{\text{final}} > I_{\max}$) and quenched to room temperature always recording the quantity $\Delta I = I_{\text{final}} - I_{\max}$. The difference between the resistance at $I_{\max}$ and just before the quenching $\Delta R = R_{\max} - R_{\text{final}}$ was also recorded. From the first order 110 $\alpha - \text{Fe}$ reflection in the XRD pattern (see Fig. 2), we calculated the average particle size $\langle d \rangle$, and the crystalline fraction ν_{cr}. Room temperature hysteresis loops were made to obtain the saturation magnetization M_s, remanence M_r, and coercive field H_c (see Fig. 3) of all annealed samples (see Table I).

TABLE I. Structural and magnetic data for $Fe_{86}Zr_7Cu_1B_6$ samples annealed at different I_{final}. No ΔR value was supplied for sample Nos. 11 and 12 because they were annealed above the $I_{2\text{nd min}}$ value.

Sample	I_{final} (A)	ΔI (A)	ΔR (Ω)	ν_{cr} (%)	$\langle d \rangle$ (nm)	H_c (A m^{-1})	M_s (T)	M_r (T)
as cast	⋯	⋯	⋯	0.0	⋯	8.0	0.30	0.10
1	1.015	0.08795	0.0275	6.9	17.1	9.0	0.43	0.17
2	1.0188	0.08821	0.0623	9.9	13.8	14.5	0.51	0.28
3	1.05	0.11737	0.1061	18.0	11.0	14.9	0.59	0.28
4	1.1096	0.18115	0.1472	21.7	9.4	13.5	0.61	0.27
5	1.1101	0.18122	0.2377	35.1	8.4	8.9	0.65	0.20
6	1.1972	0.23942	0.2770	42.8	8.8	6.2	0.80	0.27
7	1.2271	0.32819	0.3392	54.8	8.0	6.0	0.81	0.20
8	1.3192	0.3628	0.3525	63.9	7.9	5.7	0.91	0.21
9	1.3191	0.42081	0.368	68.9	8.1	4.5	0.87	0.20
10	1.4656	0.53872	0.3706	75.5	8.5	3.7	0.85	0.17
11	1.530	0.632	⋯	100	10.7	3.6	0.93	0.15
12	1.800	0.872	⋯	⋯	⋯	679	0.93	0.74

Samples in Table I were ordered by their increasing ΔI values. In the first steps of crystallization, i.e., when $I_{\text{final}} < I_{2\text{nd min}}$, ΔR and ν_{cr} increase with ΔI. This result can be understood considering that $\Delta I \propto \Delta T$ [see Fig. 1(a)] and that ν_{cr} increases with the annealing temperature. As $\Delta R = R_o(1 - \gamma \nu_{cr})^1$ (γ is a positive constant), ΔR is also expected to increase as ΔI increases. Thermal agitation becomes more important to ΔR when $\nu_{cr} \geqslant 75\%$, i.e., $I_{\text{final}} \geqslant I_{2\text{nd min}}$. The relation between the structure and the $R(I)$ curve makes ΔI a good parameter to control ν_{cr} in this system. Also, to control the crystallization process, one can play with the Joule heating rate $\delta I/\delta t$, which can be arbitrarily changed through both δI, and δt. In Fig. 1, the rate $\delta I/\delta t = 0.003\,\text{A/s}$ produced an average temperature rate of $\delta T/\delta t \approx 50\,\text{K/min}$.

Table I also shows the evolution of the average crystallite size $\langle d \rangle$. We observed that for $\nu_{cr} = 6.9\%$, $\langle d \rangle = 17.1\,\text{nm}$ and decreases down to 8.5 nm for $\nu_{cr} = 75.5\%$. This behavior can be explained as follows: the initial crystalline content is made up mainly of large Fe-rich clusters dispersed in the amorphous matrix, probably at the sample's surface.[6] As a result of the heat treatment, nucleation and growth of new crystalline clusters will rapidly occur. If the competition between these two processes favors the nucleation, there will be a limited crystalline growth, thus producing the lower $\langle d \rangle$ for higher ν_{cr}.[7] As a consequence, one should expect a broad particle size distribution at the final stages of crystallization.

From the magnetic properties presented in Table I, one sees that the coercive field H_c initially increases with ν_{cr} up to a maximum at $\nu_{cr} = 18\%$. This hardening effect can be ascribed to a small reduction in the exchange correlation length (L_{ex}). This reduction is caused by the particle size which is inversely proportional to ν_{cr}.[8] H_c reaches its low-

est value at $\nu_{cr}=100\%$. This optimum magnetic state is corroborated by a high saturation magnetization $M_s=0.93\,\mathrm{T}$, and a low remanent magnetization $M_r=0.15\,\mathrm{T}$. Sample No. 11 was quenched above $I_{2\mathrm{nd\,min}}$, and showed the best soft magnetic properties. A strong hardening was observed in sample No. 12 where the coercive field reached $678\,\mathrm{A\,m^{-1}}$ probably due to the formation of large nanocrystalline grains or borides.

In conclusion, we have shown that the LVC–JH can be used to control the structure in the $Fe_{86}Zr_7Cu_1B_6$ alloy. In particular, we demonstrated that the best soft magnetic state can be identified using the $R(I)$ curve during annealing. We find important to point out that this method can be also applied to other nanocrystalline soft magnetic alloys.

This work is supported by the Brazilian financial agencies: FAPESP, CAPES, and CNPq.

[1] P. Allia, M. Baricco, P. Tiberto, and F. Vinai, Phys. Rev. B **47**, 3118 (1993).
[2] F. C. S. da Silva, E. F. Ferrari, and M. Knobel, J. Appl. Phys. **84**, 5366 (1998).
[3] F. C. S. da Silva, E. F. Ferrari, and M. Knobel, J. Appl. Phys. **86**, 7170 (1999).
[4] J. M. Barandiarán, L. Fernéndez Barquín, J. C. Gómez Sal, P. Gorría, and A. Hernando, Solid State Commun. **88**, 75 (1993).
[5] S. N. Kaul, V. Sigururi, and G. Chandra, Phys. Rev. B **45**, 12343 (1992).
[6] D. R. Santos, I. Torriani, M. Knobel, and F. C. S. da Silva, J. Appl. Phys. **86**, 6993 (1999).
[7] H. Hermann, N. Martten, S. Roth, and P. Uebele, Phys. Rev. B **56**, 13888 (1997).
[8] A. Hernando and T. Kulik, Phys. Rev. B **49**, 7064 (1994).